

RESIDUAL NUCLIDES PRODUCED BY 290 MeV/u ^{12}C IONS BEAM IN A LIQUID WATER TARGET

J. SOLTANI-NABIPOUR¹, M.A. POPOVICI¹, GH. CATA-DANIL^{1,2}

¹Physics Department, University “Politehnica” of Bucharest, Romania,

²“Horia Hulubei”, National Institute for Physics and Nuclear Engineering,
Bucharest-Magurele, Romania

(Received March 27, 2009)

Abstract. Nowadays, heavy ion beams are used in treatment of malignant tissues. The advantageous dose profile of ion beams is partly deteriorated by the nuclear interactions with tissue nuclei, leading for example to the fragmentation of the projectiles. The experimental information on these processes is scarce and for a limited group of ions. Therefore much relies on numerical simulation of the processes. It is the goal of the present study to provide exploratory calculations for the yield and fluence of nuclear fragments produced by ^{12}C beams interacting with water target. This target is considered as first order approximation for the soft bio-tissues. For numerical simulations, a Monte Carlo approach coded in the FLUKA package has been selected.

Key words: nuclear fragmentation, dose profile, Bragg peak, residual nuclide, heavy ions.

1. INTRODUCTION

Radiation therapy with ions has become an interesting and evolving complement to photon therapy [1]. The reason is that charged particles interact with the tissues in a different way than photons, leading to a different depth dose profile. In contrast to photons, the depth dose profile of heavy charged particles is relatively small in the entrance region and reaches a maximum towards the end of their range followed by a steep decrease to almost zero values. The steep increase in energy loss was first observed for α particles by Bragg and Kleeman [3] and is known as the “Bragg peak”. A few decades later Wilson investigated the energy loss profile of protons produced at the Berkeley cyclotron [2]. He reported on a similar energy loss distribution as Bragg had observed for α particles and suggested to use protons for therapy [2]. The advantage of using protons instead of photons is primarily due to the favorable depth dose profile. Since the energy of the protons can be chosen such that the Bragg peak lies in the tumor region, the normal tissue will receive a relatively low dose. Nine years after Wilson's suggestion, the first patient receiving proton therapy was treated in Berkeley [1].

Compared to protons there are some advantages using ^{12}C ions. First, due to the mass difference, ^{12}C ions are less scattered than protons in lateral direction. This property allows irradiation closer to radiosensitive tissues. Secondly, at the end of the particle trajectory the ionization density increases, leading to clusters of lesions on the DNA-molecule in the cells. Since clusters of DNA lesions are much more difficult to repair than single DNA damages, carbon ions have an increased biological effectiveness. The properties of the ^{12}C beams make carbon especially suitable for treating deep seated, radio resistant tumors and tumors close to radiosensitive tissues [12].

When the carbon ions with energies in the MeV range penetrate in matter, they are partially fragmented due to collisions with the atomic nuclei. These collisions lead to an attenuation of the primary beam intensity and a production of secondary fragments. The fragments have longer ranges and wider energy distributions than incident ions producing a characteristic dose tail behind the Bragg Peak. It is known also that the biological effect of energetic ions radiation is dependent on the particle field composition. For these reasons a detailed knowledge of the nuclear fragment production is important in order to obtain an accurate dosimetric evaluation. In particular, understanding the fragmentation of the beam projectiles in high energetic nucleus-nucleus interactions is a very important issue for heavy ion radiotherapy [4]. The projectile fragmentation products can cause an undesired dose beyond the Bragg Peak, which leads to an unwanted dose delivered to the healthy tissues. This effect can be estimated if the residual nuclides of carbon ions in tissue equivalent materials, e.g., water, are known. However, the fragmentation of carbon ions is not yet fully understood. Several measurements of fragmentation of carbon ions in water and tissue like materials have been performed but when compared to the predictions of nuclear models, significant discrepancies are observed [5]. Moreover, measurements of geometrical distribution of the carbon fragments are scarce. More calculations and experimental information are therefore needed to better understand the nuclear fragment production in biological matter by carbon and other heavy ions.

In the present study it was considered a liquid water targets as a commonly adopted simplified model for soft tissues and has been calculated the nuclear fragments production induced by a 290 MeV/u ^{12}C beam. Discussions are extended on the distributions of the fluence and yield of the nuclear fragments with beam energy and geometrical coordinates on the target. The calculations have been performed with FLUKA simulation code in a Monte Carlo approach.

2. ENERGY LOSS OF CHARGED PARTICLES IN MATTER

Heavy charged particles interact primarily through elastic and inelastic collisions with electrons and nuclei [7]. The most important processes for the

energy loss are the inelastic collisions with electrons, leading to excitation or ionization of the target atoms.

The collisions are statistical processes but the number of interactions is in general large, therefore one can work with the average energy loss [6]. The average energy loss per unit path length stopping power due to inelastic collisions with electrons was first calculated by Bohr using classical arguments. Nowadays, the Bethe-Bloch equation (1) which is a semi-classical description of the stopping power is widely employed [7, 8, 9]:

$$-\frac{dE}{dx} = \frac{4\pi e^4 Z_t}{m_e c^2 \beta^2} Z_p^2 \left[\ln \frac{2m_e c^2 \beta^2}{\langle I \rangle (1-\beta^2)} - \beta^2 \right] + (\text{corrections}), \quad (1)$$

where m_e is the rest mass of the electron, $\beta = V/c$, V the velocity of projectile, Z_p the atomic number of the projectile, Z_t the atomic number of the target and $\langle I \rangle$ the mean ionization potential of the target material.

Near the end of the trajectory, when the velocity is of the order of the Bohr velocity, the projectiles start picking up electrons. Then the nuclear charge, Z_p in the Bethe-Bloch equation (1), has to be replaced by an effective charge Z_{peff} . The Z_{peff} can be approximated by the Barkas formula [9]:

$$Z_{peff} \cong Z_p \left(1 - e^{-125\beta Z_p} \right). \quad (2)$$

At lower energies the energy loss rises due to the $1/V^2$ dependence. But after a maximum, dE/dx will decrease and not diverge, due to the Z_{peff} behavior. For decreasing energy the Z_{peff} approaches zero, producing a sharp peak in the energy (Bragg peak) of which ion therapy makes use. The energy loss is proportional to the charge of the projectile squared, Z_p^2 and is not dependent on its mass. This means that the energy loss of a carbon ion will be 36 times higher than the energy loss of a proton of equal velocity.

The range R of a particle with kinetic energy T can be determined through integration of the inverse energy loss function over the energy.

$$R = \int_0^T \left(\frac{dE}{dx} \right)^{-1} dE. \quad (3)$$

In Ref. [12] and [13] it is shown that for particles with same velocity the range is in a good approximation proportional to A/Z_p^2 . This means that fragments with smaller Z will have longer ranges than those with higher atomic number (including the incident beam), providing a simple explanation for the experimental fact that fragments give rise to a dose tail behind the Bragg Peak.

In the present study, the penetration depth of ^{12}C ions beam and the corresponding energy values in a cylindrical ($R = 10$ cm, $H = 40$ cm) water target were calculated and graphically represented.

3. FRAGMENTATION

Heavy charged particles penetrating matter do not just loose energy through inelastic collisions with the target electrons. They might be involved in nuclear reactions, for example, where the primary particles are subject to fragmentation collisions which decrease the number of primaries with the corresponding increase of lighter fragments along the penetration path [11].

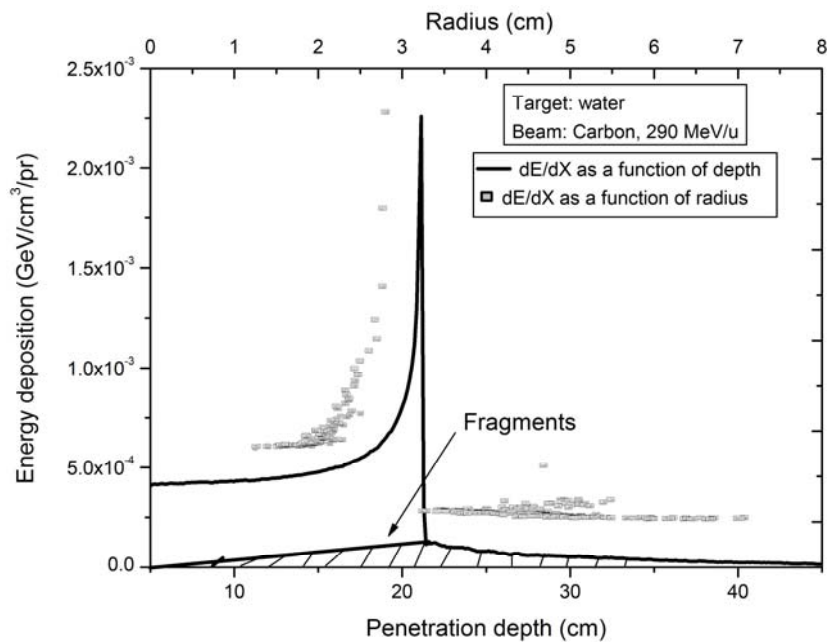


Fig. 1 – Dose profile of carbon ions beam as a function of penetration depth (continuous curve) and radius (scatter points) in a cylindrical ($R = 10$ cm, $H = 40$ cm) water target. The contribution of the beam fragmentation product is indicated in dash area. The computations have been performed within a Monte Carlo model coded in FLUKA computer code.

High energy projectiles can be described as particles that move on straight lines through the target and from time to time a target nucleus lies on this line and causes a nuclear collision.

At high energies ($E > 0.100$ MeV/u) the cross section for a nuclear reaction is primarily determined by the geometrical dimensions of the projectile and target nuclei as it is considered for example in a simple abrasion-ablation model [14].

Consider an ion beam moving in the x direction. Then the number of ions, N , remaining after the beam interacts with the target over a distance x is given by:

$$N(x) = N_0 e^{-x/\lambda}, \quad (4)$$

where λ is a material constant known as mean free path, and N_0 is the incident number of ions.

A few centimeters before the Bragg peak, the decrease escalates and ends up in a steep fall behind the Bragg peak. The fraction of primary ions reaching the Bragg peak is approximately 70% for the 0.200 MeV/u and 30% for the 0.400 MeV/u ^{12}C beams [14]. Therefore, the loss of carbon ions and the build-up of fragments due to inelastic collisions with target nuclei cannot be neglected. Table 1 shows the production of residual nuclei and their yield by a 290 MeV/u ^{12}C ion beam in water as obtained from the present calculations.

Table 1

Predicted isotope yields of residual nuclides produced by 290 MeV/A ^{12}C ions beam in a water target. The yields are given as average number of residual nuclei produced per cm^3 of target material by one projectile. The calculations have been performed with the FLUKA package

Isotope yield (nuclei / cm^3 / pr)	Atomic mass number (A)	Atomic number (Z) and corresponding yield
3.86E+01	1	1
3.33E+01	2	1
2.66E-01	3	1(0.084), 2(0.182)
1.21E+00	4	2
0.00E+00	5	3
7.90E-02	6	2(0.0055), 3(0.0735)
7.65E-02	7	3(0.038), 4(0.385)
1.50E-02	8	2(0.005), 3(0.008), 5(0.0065)
2.90E-02	9	3(0.001), 4(0.027), 6(0.001)
6.55E-02	10	4(0.0105), 5(0.45), 6(0.01)
1.67E-01	11	4(0.0005), 5(0.086), 6(0.0805)
7.46E-01	12	5(0.0065), 6(0.73873), 7(0.0005)
8.16E-02	13	5(0.0005), 6(0.716299), 7(0.0095)
1.15E-01	14	6(0.0155), 7(0.094), 8(0.0055)
3.44E-01	15	7(0.208464), 8(0.136)
6.55E-02	16	7(0.00504521), 8(0.0604146)
5.51E-05	17	8

4. YIELD AND FLUENCE OF THE FRAGMENTS PRODUCED IN WATER

In the first part of the beam trajectory inside the target where most of the ^{12}C ions are still present, the fragment production such as ^{10}B is high and its yield increases steeply [14]. The yield is defined as the number of fragments produced

per primary ^{12}C ion. The fragment yield can be obtained by integration of their angular distributions along the polar angles (θ, φ) as follow:

$$Y = \int_0^{2\pi} \int_0^{\pi} f(\theta) \sin(\theta) d\theta d\varphi = 2\pi \int_0^{\pi} f(\theta) \sin(\theta) d\theta, \quad (5)$$

where $f(\theta)$ is the angular distribution expressed as number of fragments per primary particles per steradian and a cylindrical symmetry was assumed.

The amount of charged fragments increases with penetration depth, reaching a maximum in the Bragg peak region, as illustrated in Fig. 1. Behind the Bragg peak the amount of fragments drops since all carbon ions have stopped and cannot produce new fragments. Lighter fragments, which in general have longer ranges, can still be produced from heavier fragments. For instance, hydrogen and helium nuclei are produced most frequently (Table 1). The yield of heavier fragments like boron, beryllium and lithium is about one order of magnitude smaller.

Figure 2 shows the fluence of heavy ions production as a function of energy for 290MeV/u ^{12}C ions beam in water obtained in the present simulation. The number of carbon ions considered in the Monte Carlo trials was 10^4 , and the beam diameter (d) was neglected (narrow pencil beam). A cylindrical geometry for the target with the incident beam directed along its axis has been selected for this study.

As can be observed from Fig. 2, at the entrance of the projectile in water certain dispersion in the fluence of heavy ion fragments occurs. With the decreasing of the beam energy this dispersion becomes less important and it diminished for energies

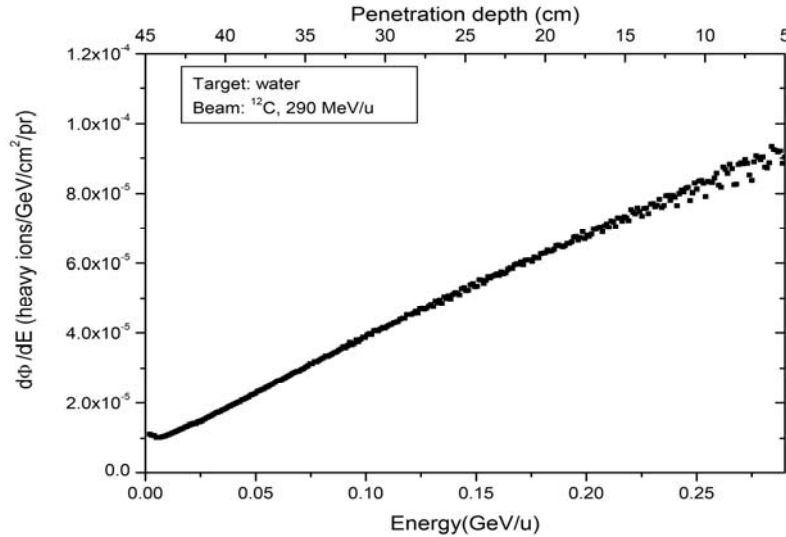


Fig. 2 – Fluence of heavy ions produced by ^{12}C ions beam induced in water as a function of beam energy. See text for comments. Calculations were performed in the same conditions as given in Fig [1].

smaller than about 0.200 MeV/u corresponding to 16 cm in penetration depth. The subsequent decrease of fluence with energy is practically linear. It should be noticed that in FLUKA [15] all ions are identified as particles with the same “id” number (-2) corresponding to heavy ions. Therefore Fig. 2 refers to all ions obtained in the present calculation.

Figure 3 shows the fluence of protons produced by a beam of 290 MeV/u ^{12}C in water. At the entrance of the projectile in the target, the proton fluence is 2.0×10^{-3} protons/GeV/cm² per primary particles which is relatively low compared to the average fluence along the entire trajectory. Then it increases up to a maximum value at 9.0×10^{-3} protons/GeV/cm² per primary particles corresponding to an energy value of 75 MeV/u, and a penetration depth of 35 cm. When the projectile energy decreases below 75 MeV/u, the protons fluence decreases as well and its value falls to 2.0×10^{-3} protons/GeV/cm² per primary particles. Overall the magnitude of fluence for protons ranges between $2.0 \times 10^{-3} - 9.0 \times 10^{-3}$ protons/GeV/cm² per primary particles. The expected uncertainties of the calculations are of the order of symbol size.

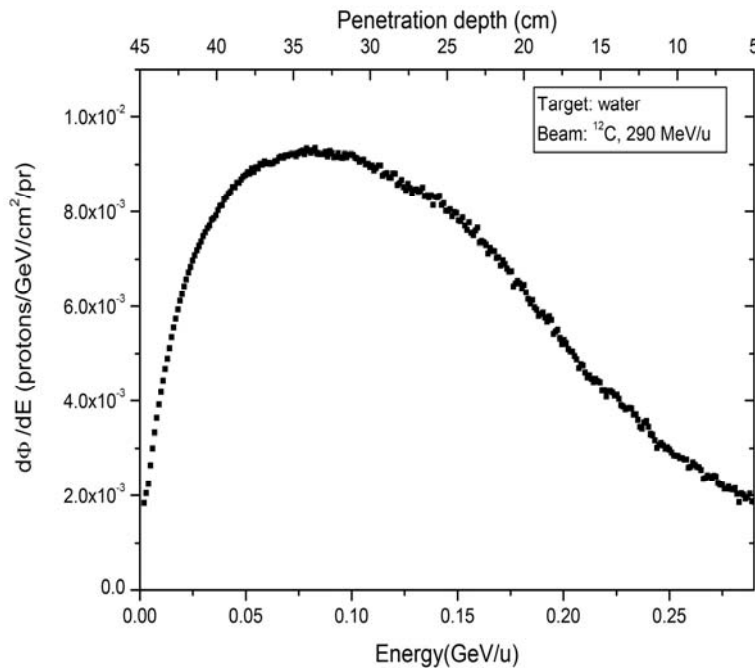


Fig. 3 – Fluence of protons produced by ^{12}C ions beam induced in water as a function of energy and penetration depth. Calculations were performed in the conditions given in Fig [1].

Figure 4 shows the fluence of neutrons in water as a function of beam energy and penetration depth. At the entrance, neutron fluence is 7.5×10^{-3} neutrons/GeV/cm² per primary particles which is more than three times order

magnitude higher than proton fluence under the same depth. However the increase in the neutron fluence does not exhibit a maximum as in the proton case. In fact the neutron fluence increases almost monotonously and reaches some local maximum at the energy of 150 MeV/u corresponding to 1.3×10^{-2} neutrons/GeV/cm² per primary particles. This can be produced by secondary reactions with high cross section for neutron emission. The fluence of neutrons ranges between 4.0×10^{-3} – 2.5×10^{-2} neutrons/GeV/cm² per primary particles, as presented in Fig. 4.

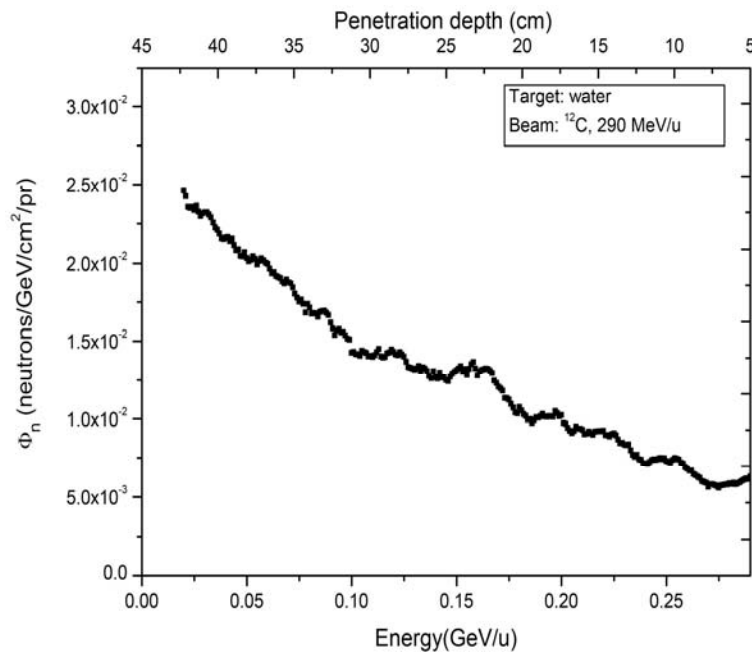


Fig. 4 – Fluence of neutrons produced by ¹²C ions beam induced in as a function of energy. Calculations were performed in the conditions given in Fig [1].

Similar with the heavy ions case, the deuteron fluence, presented in Fig. 5, exhibits a constant decrease with the penetration depth. The deuterons fluence at entrance is 8.0×10^{-4} deuterons/GeV/cm² per primary particles which is very low as compared to the entrance protons and neutrons fluence. The fluence of deuterons falls to 1.0×10^{-4} deuterons/GeV/cm² per primary particles at the end of the beam trajectory. The fluence decreases almost monotonously and reaches some local maximum at 275 MeV/u which is near to the entrance value, corresponding to 8.0×10^{-4} deuterons/GeV/cm² per primary particles. Moreover, the fluence exhibits some local minimum at 225 MeV/u, corresponding to 6.0×10^{-4} deuterons/GeV/cm² per primary particles. A particular feature that can be observed from Fig. 5, across a length which is more than half of the length of the cylindrical target this decrease is accompanied by a significant scattering of the calculated values.

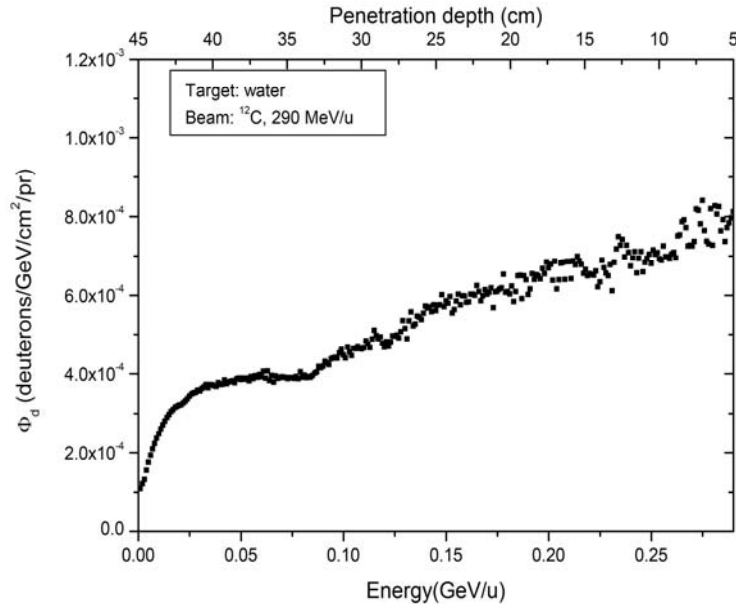


Fig. 5 – Fluence of deuterons produced by ^{12}C ions beam induced in water as a function of the beam energy (lower scale) and penetration depth (upper scale). Calculations were performed in the same conditions as given in Fig [1].

5. CONCLUSIONS

In the present work have been calculated fluence and yield of the nuclear fragments produced in the interaction of 290 MeV/u ^{12}C ions beam with a water target. In the numerical simulations was employed a Monte Carlo model coded in FLUKA package.

The energy deposition along the axial (incident beam direction) and radial directions of a cylindrical target was evaluated. The results show that in the radial direction a peak value is obtained at about 3 cm apart the cylinder axis. This result indicates a significant spreading of the projectile and fragment trajectories corresponding to a penetration depth slightly shorter than those of the Bragg peak position. The energy deposition along the beam trajectory and beyond the Bragg peak due to nuclear fragments has been calculated in detail.

The yield of all nuclear fragments originating directly from ^{12}C projectiles and from secondary products was obtained in this study. The calculations indicate that the main components of this yield are produced by protons and deuterons.

Another observable calculated in this work was the fluence of fragments such as protons, neutrons, deuterons and heavy ions along the entire trajectory of the projectile inside the target. Also, it outlines the fact that the behavior of fluence versus energy is different for the main types of fragments, as qualitatively expected.

Since medium mass heavy ions with energy in the range 200-400 MeV/u are in use or are proposed to be used in hadronotherapy at several facilities worldwide, further detailed studies concerning the yields of nuclear products produced by these ions are necessary. Finally, the present calculations show that build-up of nuclear fragments should be carefully considered in order to get information on possible unwanted dose delivered to healthy tissues near the projectile trajectory.

REFERENCES

1. J. Sisterson, *A Newsletter for those Interested in Proton Light Ion and Heavy Charged Particle Radiotherapy*, Particles, **35**, 11 (2005).
2. R. Wilson, *Radiological use of fast protons*, Radiology, **47**, 487–491 (1946).
3. W. Bragg, R. Kleeman, *On the α particles of radium and their loss of range in passing through various atoms molecules*, Phil. Mag., **10**, 318–340 (1905).
4. P.L. Petti and A.J. Lennox, *Annu. Nucl. Part. Sci.*, **44**, 155 (1994).
5. A.N. Golovchenko et al., *Total charge-changing and partial cross-section measurements in reactions of 100-250 MeV/nucleon ^{12}C in carbon, paraffin and water*, Physical Review, **C66** (2002).
6. R.D. Evans, *The Atomic Nucleus*, Mc Graw-Hill, 1955.
7. H. Bethe, *Zur Theorie des Durchgangs schneller Korpuskularstrahlung durch Materie*, Ann. Phys. (Leipzig), **5**, 325–400 (1930).
8. F. Bloch, *Bremsvermögen von Atomen mit mehreren Elektronen*, Z. Phys., **81**, 136–154 (1933).
9. F. Bloch, *Zur Bremsung rasch bewegter Teilchen beim Durchgang durch Materie*, Ann. Phys. (Leipzig), **16**, 285–321 (1933).
10. W. Barkas, *Nuclear Research Emulsions*, Vol. 1, Academic Press, New York, London, 1963.
11. A.S. Goldhaber and H.H. Heckman, *Ann. Rev. Nucl. Part. Sci.*, **28**, 161–205 (1978).
12. J. Soltani-Nabipour, Gh. Cata-Danil, *Monte Carlo computation of the energy deposited by heavy charged particles in soft and hard tissues*, U.P.B. Sci. Bull., Series A, **70**, 3, 73–84 (2008).
13. J. Soltani-Nabipour, D. Sardari, Gh. Cata-Danil, *Sensitivity of the Bragg peak curve to the average ionization potential of the stopping medium*, Romanian Journal of Physics, **54**, 3–4, 321–330 (2009).
14. E. Haettner, *Experimental study on carbon ion fragmentation in water using GSI therapy beams*, Master thesis, 2006.
15. www.fluka.org